

Mouse embryonic stage (number of somites)

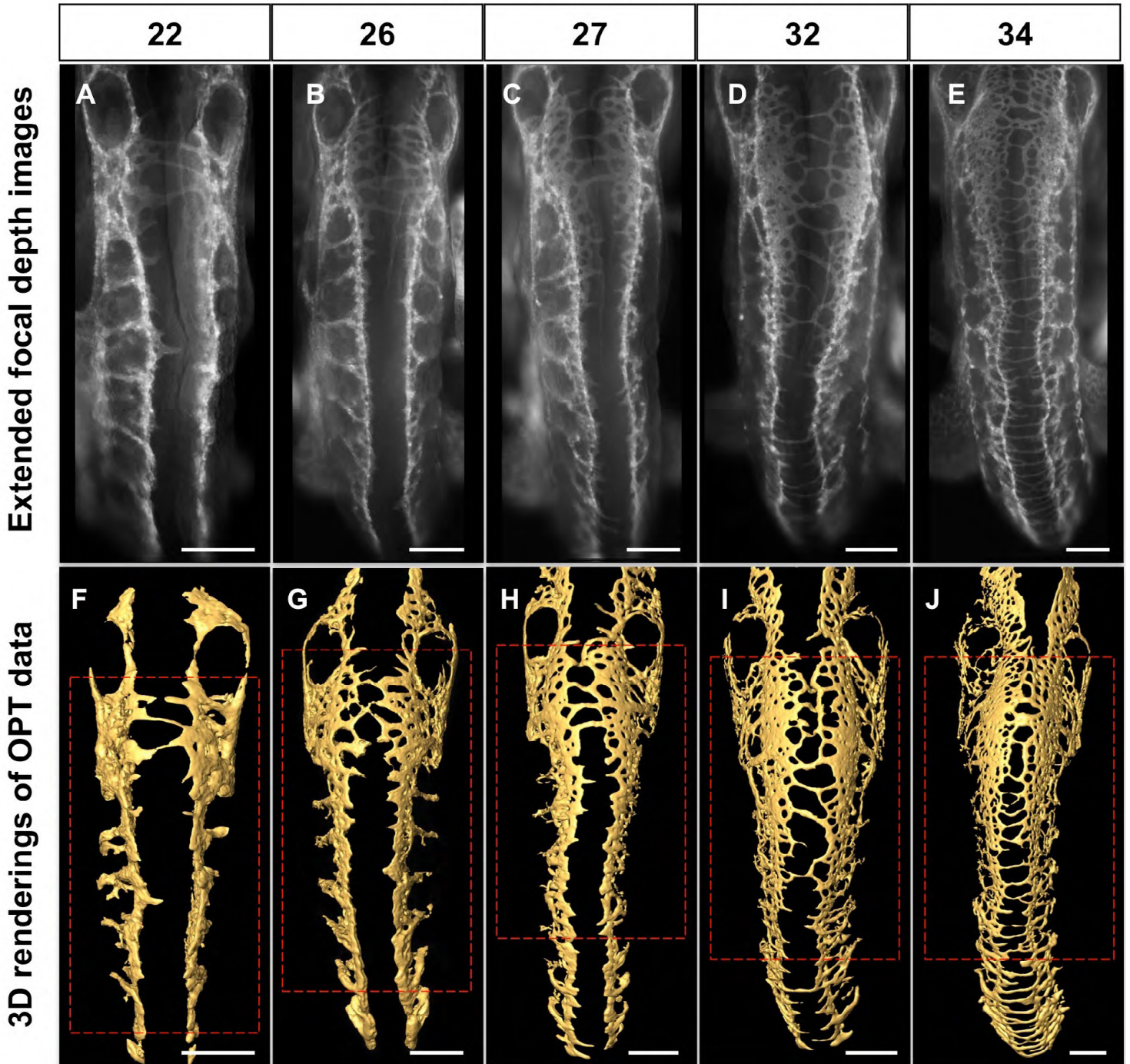


Fig. S1. DLAV plexus morphogenesis in mouse embryos. (A-J) Dorsal views of DLAV plexus development in 22 (A,F), 26 (B,G), 27 (C,H), 32 (D,I) and 34 (E,J)-somite stage Swiss-Webster wild-type mouse embryos. Anterior, top. Scale bars: 250 μ m. (A-E) PECAM-1 immunofluorescence. Endothelium, white. (F-J) 3D-rendered OPT data (see Materials and Methods) collected from the same embryos. Endothelium, gold. Red dashed lines denote cropped regions displayed in Fig. 1Q-U.

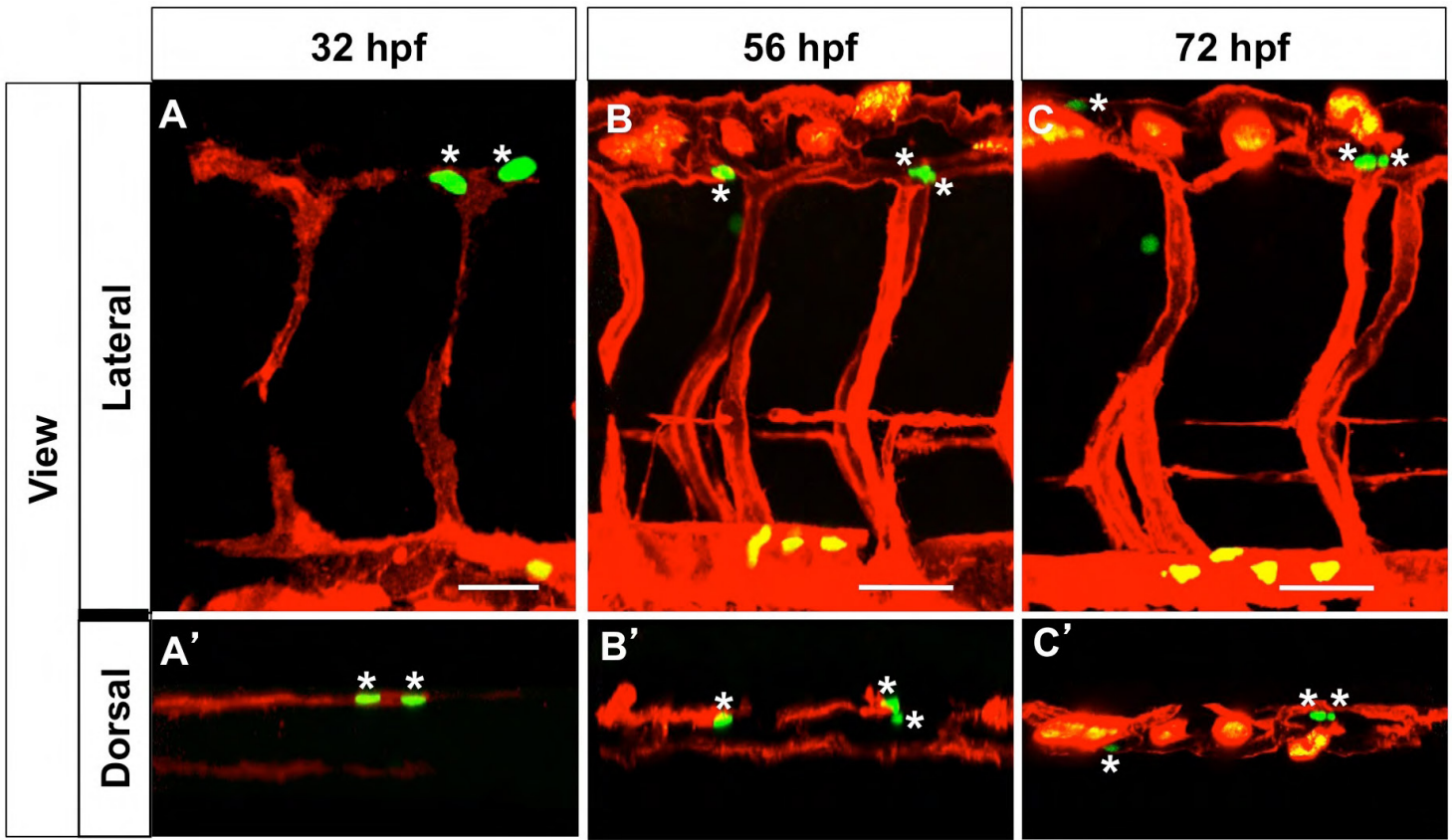


Fig. S2. Endothelial cell proliferation contributes to DLAV plexus morphogenesis. Lateral (A-C; dorsal, up) and dorsal (A'-C') images of the trunk vasculature of a chimeric embryo made from a *Tg(flk1:EGFP-NLS)* donor and a *Tg(flk1:ras-mCherry)^{s896}* host at 32 (A-A'), 56 (B-B'), and 72 (C-C') hpf. Anterior, left. White asterisks, endothelial cell nuclei of donor origin found within the DLAVs and/or DLAV plexus. (A-C') Endothelium, red. Endothelial cell nuclei, green. Scale bars: 30 μ m.

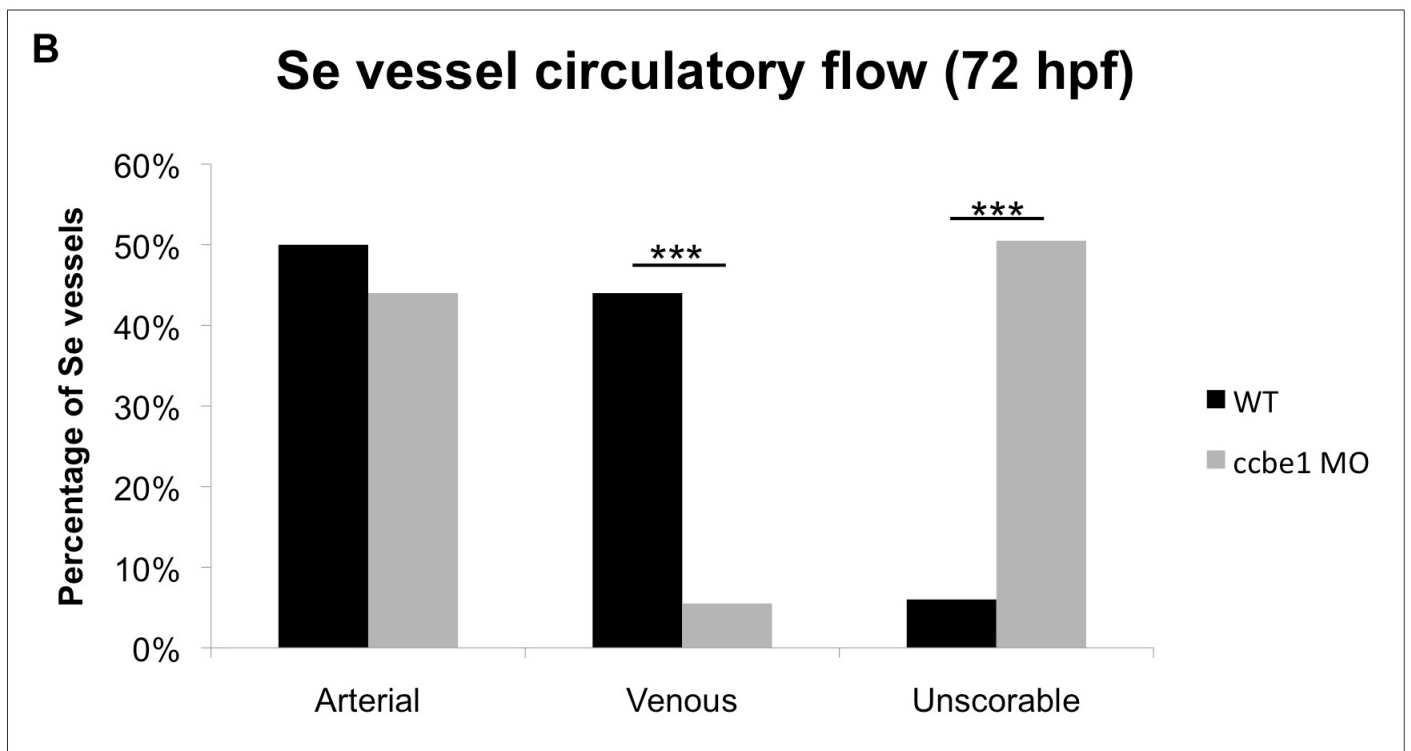
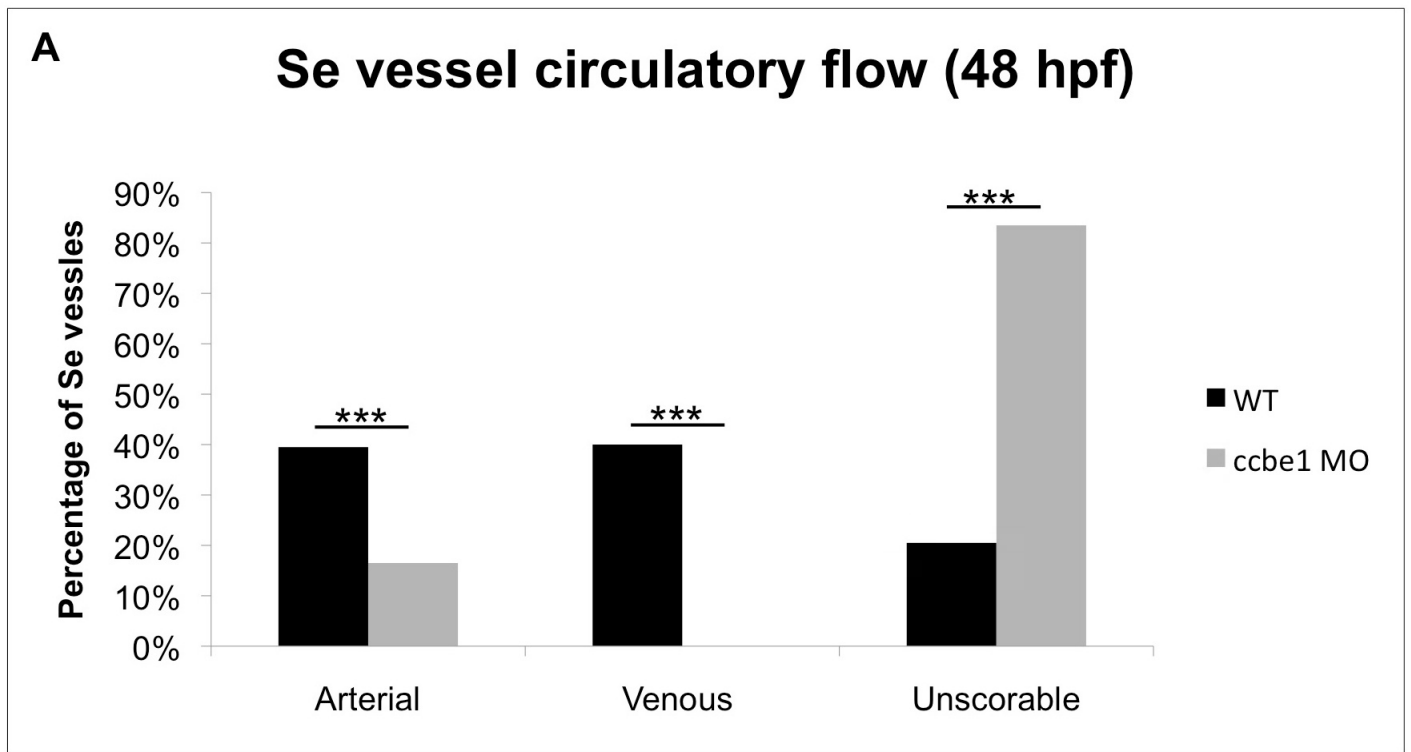


Fig. S3. The percentage of Se vessels carrying venous flow is dramatically reduced in *ccbe1* morphants. Quantification. Arterial and venous flow through Se vessels in WT and *ccbe1* morphants (*ccbe1* MO) at 48 (A) and 72 (B) hpf. $n=20$ animals per condition and stage. *** $P<0.001$.

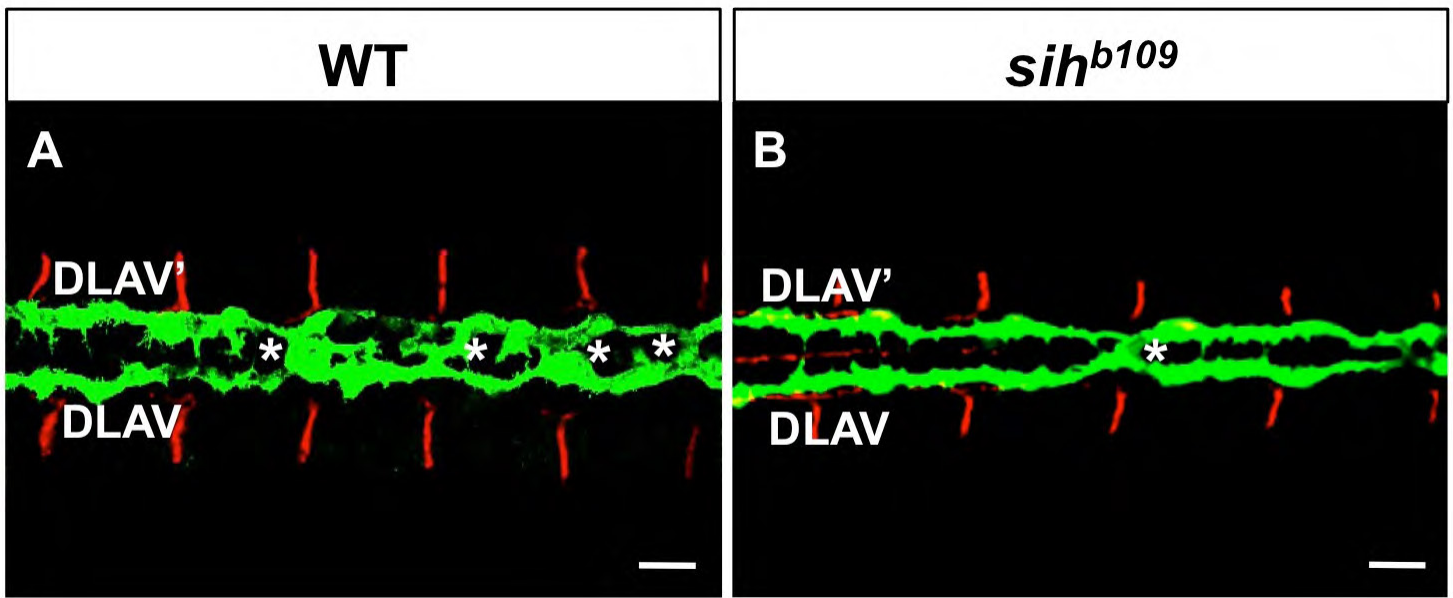


Fig. S4. Circulatory flow promotes DLA V plexus formation. (A,B) Dorsal views of the trunk vasculature of 48 hpf WT (A) and *sih*^{b109} mutant (B) *Tg(fli:EGFP)^{v1}* embryos. Anterior, left. White asterisks, contra-lateral DLA V interconnections. Endothelium, green. Somite boundaries, red. Scale bars: 30 μ m.

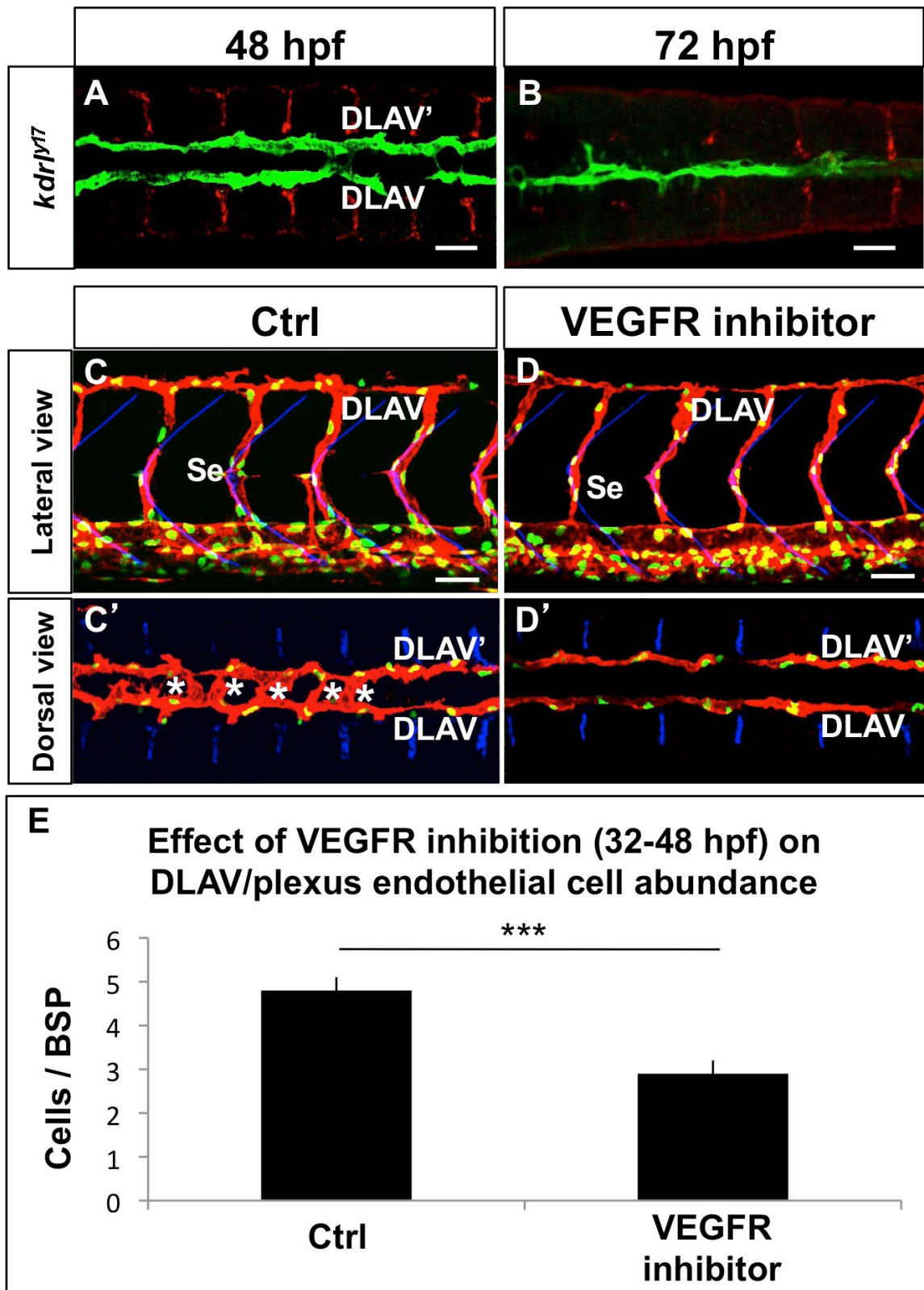


Fig. S5. Lack of VEGF signaling prevents the initiation of DLAV plexus formation. (A,B) Dorsal views of the trunk vasculature of 48 (A) and 72 (B) hpf *kdr^{fl/y17}; Tg(fli:EGFP)^{y1}* mutant embryos. Note lack of DLAV plexus formation. Anterior, left. (C-D') Lateral (C,D) and dorsal (C',D') views of the mid trunk vasculature of 48 hpf *Tg(flk1:EGFP-NLS); Tg(flk1:ras-mCherry)^{s896}* embryos treated post-DLAV formation (32 hpf onwards) with either vehicle (Ctrl; DMSO) or with VEGFR inhibitor (SU5416). (A-D') Anterior, left; dorsal, up; endothelium, green (A,B) or red (C-D'); endothelial cell nuclei, green (C-D'); somite boundaries, red (A,B) or blue (C-D'); scale bars: 30 μ m. (E) Quantification of the effect of VEGFR inhibition (32-48 hpf) on DLAV and/or DLAV plexus endothelial cell abundance. $n=10$ animals per treatment. Error bars, s.e.m. *** $P<0.001$.

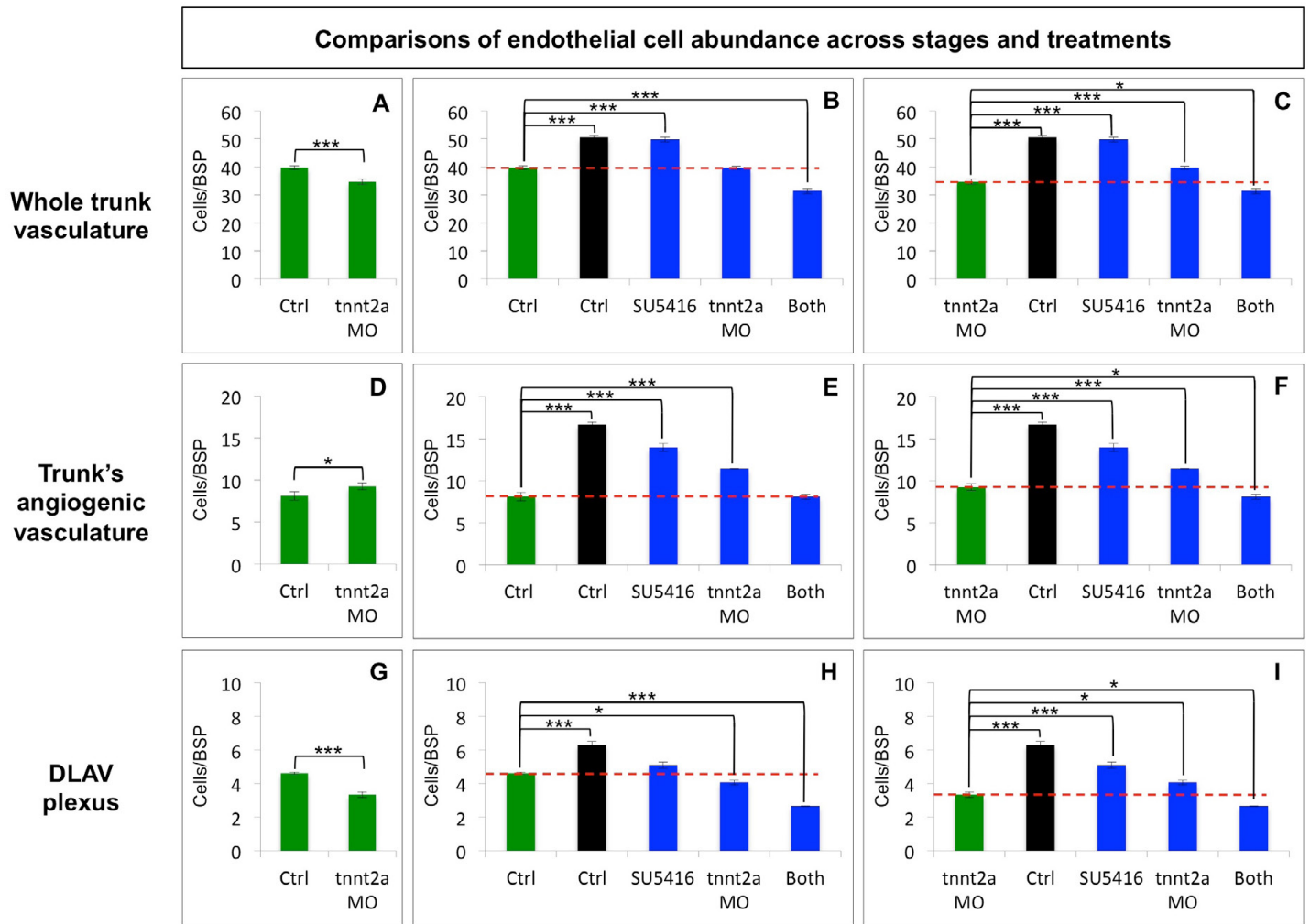


Fig. S6. Additive effects of VEGF signaling and circulatory flow on DLAV plexus development and maintenance. (A-I) Quantifications of the vasculature of *Tg(flk1:EGFP-NLS)*; *Tg(flk1:ras-mCherry)^{s896}* embryos. 43 hpf, green bars (ctrl and *tnnt2a* morphants); 56 hpf, black (ctrl) or blue bars (experimental conditions); as in Fig. 4 (see Materials and Methods). The red dotted lines (at the level of the corresponding 43 hpf value) are included to facilitate comparisons. $n=6-10$ animals per treatment and stage. Error bars, s.e.m. * $P<0.5$; *** $P<0.001$.